Lawrence Livermore Laboratory

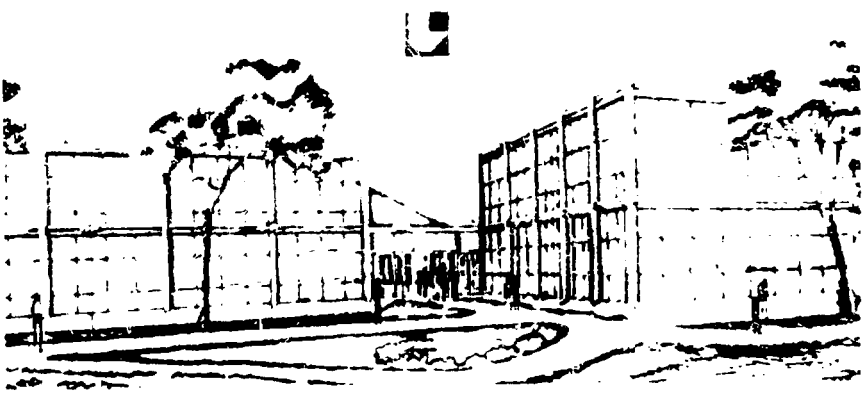

ANALYSIS OF DENSE PUSHER LASER DRIVEN IMPLOSIONS FOR INTERMEDIATE DENSITIES*

W.C. Mead, [illegible].D. Orth, [illegible].S. Ba[illegible]ley,

G. McClellan, and K.G. Estabrook

University of California, Lawrence Livermore Laboratory,

Livermore, California 94550

ABSTRACT

We report [illegible] analysis of [illegible] compression of DT gas to [illegible] density. The SHIVA laser [illegible]. Details of comparisons of [illegible] with [illegible]. Implications [illegible] parameters [illegible] analyzed. [illegible] strong support for the [illegible] program.

*Work performed under the auspices of the U.S. Department of Energy by the Lawrence Livermore Laboratory under contract number W-7405-ENG-48.

[1]Experiments with Polymer Coated Microspheres Irradiated by the SHIVA Laser System, J. M. Auerbach, K. R. Manes, D. [illegible]. Matthews, [illegible]. N. Koppel, S. M. Lane, E. M. Campbell, N. M. Ceglio, D. W. Ph[illegible], R. H. Y. Lee, V. C. Rupert, D. [illegible]. Banner, E. D. Swift, [illegible]. W. Hatcher, and W. C. Mead, Bull. Am. Phys. Soc. [illegible], 10[illegible] (197[illegible]).

diagnostics employed to allow inference of the DT density achieved: x-ray continuum imaging, imaging of line emission produced by Ar seeded in the fuel, and radiochemical activation of the ^{28}Si in the glass pusher material. Section IV presents a brief summary of the results and an indication of some possible future directions.

Throughout this report, the symbol $\langle \dot{n} \rangle_r$ is used to denote

$$\langle \dot{n} \rangle_r = \iint \dot{n} \, dr \, dt \Big/ \int \dot{n} \, dt$$

where $\dot{n}$ is the neutron production rate and the spatial integration is over the pusher material.

ABSORPTION/SCATTERING

Based on previous experiments, much of the light absorption at intensities of 10^{16} W/cm^2 occurs via collective plasma processes, mainly resonant absorption at the critical surface [1,5]. Angle- and polarization-dependent absorption measurements have shown ~40% absorption at $1-4 \times 10^{15}$ W/cm^2, for incidence at 30 degrees with P polarized light [6]. In order to enhance resonant absorption as much as possible, the OMEGA beams were designed to illuminate planar targets with P polarized light by orienting the electric field vector of each beam radially.

In the OMEGA 16 X "Ball-on-Stalk" target experiments, the absorption was measured on two shots using both optical and plasma calorimetry. The best absorption value is taken as [illegible]

The high energy heated electrons produced by resonant absorption give rise via their bremsstrahlung to a characteristic suprathermal x-ray tail. The experimental measurement of this tail for the 16 X target was complicated by neutron-induced background in the Filter/Fluoresced detector system [3]. A special shot had to be fired using a target ball without DT fill. A further, more fundamental difficulty encountered was an apparent strong angular modulation of the high energy x-ray emission [8]. The origin of this modulation of a factor 5:1 (peak-to-valley) is not understood at present. As a result, we are forced to include error bars of a factor of 4 on the otherwise-precise Filter/Fluoresced x-ray measurements.

For the 10 X designs discussed here, the Brillouin scattering level is calculated to be comparable (Fig. 1). The estimated 30-50% loss to stimulated Brillouin scattering, together with expected resonant absorption of ~30%, can reasonably account for the experimentally observed 45 - 50 % net absorption. More data on experiments are required to determine the mix of absorption/scattering processes more precisely.

TRANSPORT

The calculations presented here use multigroup flux-limited diffusion to transport the suprathermal electrons and a plasma-wave model for the thermal electrons are transported by a single Maxwellian group.

In accordance with modeling of previous experiments [ ], the fraction of energy carried by thermal electrons was reduced using the two-stream model of Max and Estabrook [ ]. As a typical example, for T_e = 2 keV in the general plasma regime, $\nu_{ei}/\omega_p \approx 0.1$, the wave-particle interaction produced by the two-stream mode will typically result in a limit of f=0.03 times the normal free streaming flux. This reduced flux limit on thermal electron power flow will typically result in a factor of order 2 for this design. Further experiments will test the suitability of the modelling for these 10 x experiments.

temperatures occur before the maximum fuel compression. This mistiming is design- and model- dependent. Its impact on the density achieved and inferred is discussed in section III.

Note that the velocity of the pusher/fuel boundary is sharply reduced during the last phase of compression by a shock reflected from the explosion center. Since the dense pusher is being decelerated by the lower density fuel, the fuel/pusher interface can suffer significant growth of spatial perturbations of various wavelength by Rayleigh-Taylor instabilities. This can result in significant mixing of the cooler, higher-Z pusher into the fuel, lowering the fuel temperature, and reducing the burn rate. A crude estimate of the burn reduction caused by this mechanism is obtained by treating the fuel mix as the line marking the continuation of the pusher profile towards the origin. When the fuel is reduced to 70% of its current fuel radius, burn is considered cut-off. The "no-mix" yield value quoted here is the "full-mix" yield multiplied by 1.5. In target modelling, the mix-correction reduces the calculated yield by a factor of 1.5-5. The quantitative evaluation of mix effects in an asymmetric 3-dimensional implosion is a complex subject worthy of considerable future investigation.

Figure 8 shows the plasma profiles at the time of peak compression. Note that even though this is after the burn is over, the glass pusher is still not entirely assembled as a constant-density shell around the fuel. This has impact on the various density diagnostic discussed below.

Intermediate Density Tests

[illegible]

Figure 11 shows plasma density and temperature contour plots for the two-stream-only calculation. Two post-processor calculated sca

[illegible] more detailed information.

[illegible]

[illegible] concept of the proton model for [illegible] the proton [illegible] of two [illegible] [illegible] experiment [illegible] the proton [illegible] model dependent way [illegible] However, we would like to [illegible] model dependence which [illegible] data for the [illegible]

A [illegible] rotating [illegible] the [illegible] for [illegible] providing the [illegible] condition around the [illegible] the fraction of the proton [illegible] thin constant-density [illegible] model dependent feature of the activated proton as [illegible] initially. This model dependence can be [illegible]

[illegible] T_{ion} [illegible] by factor of 2 and T_e [illegible] equal to T_{ion} [illegible] would be increased by factor of 2 and specific heat by factor of 2, electron-ion coupling decreased by factor of [illegible] thermal electron conductivity enhanced and reduced by a factor of [illegible] from the nominal [illegible] value. The [illegible] order of magnitude, and [illegible] the experimental [illegible] [illegible] effects [illegible].

In order to be conservative in [illegible] the range depends on the relationship between effective pusher [illegible] and the [illegible] one of these could be true at [illegible] time point in fuel density [illegible] plotted in Fig. 2. The total uncertainty [illegible] mode variation [illegible] factor of 3 [illegible] density at peak burn or "bang" time. The [illegible] density at peak compression [illegible] The most sensitive [illegible] electron conductivity during the [illegible] conduction to the pusher. The [illegible] model-dependence are [illegible] the rather [illegible] most effectively activated pusher material [illegible] and this is the material responsible for [illegible] most changes in implosion condition which modify the fuel [illegible] reflected by changes in pusher [illegible]

IV. SUMMARY AND POTENTIAL FUTURE DIRECTIONS

The results presented here have shown that the fabrication of a number of design/experimental/technical issues. Fabrication of glass microballoon and coated microspheres has become a well-established part of multiple diagnostics to determine the implosion fuel information is established. We have discussed the model-predictions of three potential density diagnostics. The x-ray images and radiochemical activation of the pusher or, preferably, a high-Z material in the fuel, offer the most quantitative information about fuel density.

Furthermore, taken together, the results of experiment and calculation form a rather convincing case that the 5-10 micron target performance is collectively the result of the effects of mix rather than inadequate drive symmetry or liquid density. The x-ray continuum images are not very well resolved but which reach 10-16 x liquid density. Images of the core show stagnating core dimensions consistent with calculations in the 1-12 X range. Radiochemical activation of the pusher material or "mix" time fuel densities of 5-11 X can be detected exceeding 10 X L.D. are quite likely.

Improved heating uniformity and stagnated core symmetry were obtained with the "Ball-in-Plate" configuration. The neutron yield

Thanks are due to [illegible] for support and useful discussions.

8. C. . Wang, H. N. Kornblum and V. W. Slivinsky, Bull. Am. Phys. Soc. 24, 1106(1979).

9. M. J. Boyle, European Conference on Laser Interaction with Matter, Oxford, England (1977); and M. J. Boyle, D. T. Attwood, W. M. Cox, D. L. N. Koppel, V. W. Slivinsky, J. T. Larsen, F. K. Storm, R. H. Price and H. G. Ahlstrom, Univ. of Calif. Report UCRL-79817 (1977).

10. W. F. Cohen and C. E. Max, Phys. Fluids 22, 1115 (1979); D. W. Phillion, W. L. Kruer and V. C. Rupert, Phys. Rev. Lett. 39, 1529 (1977).

11. V. W. Slivinsky, Univ. of Calif. Report UCRL-50021-77, p. 2-55 (1977).

MAXIMUM AVERAGE DENSITY

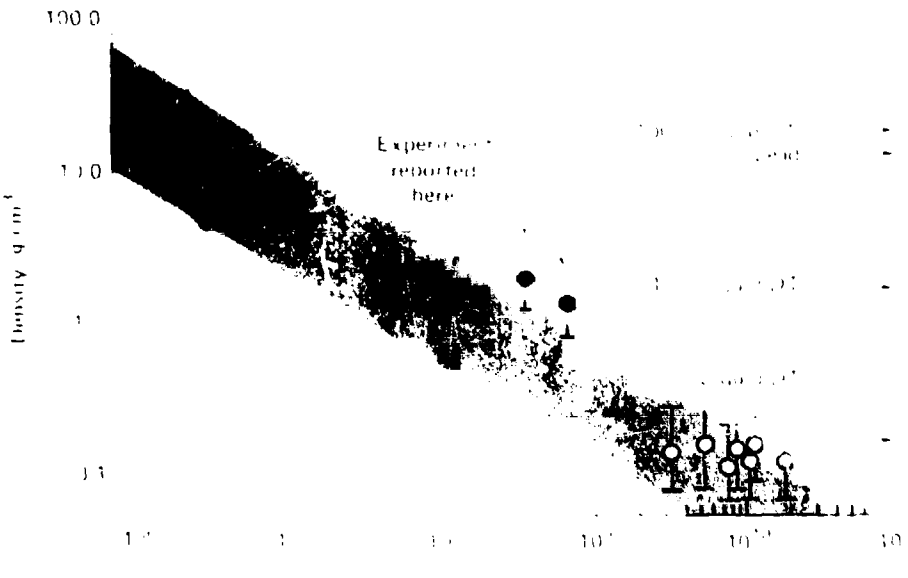

02 30 1-79 4364

"10X" BALL/BALL-IN-PLATE TARGET DESIGN FOR SHIVA

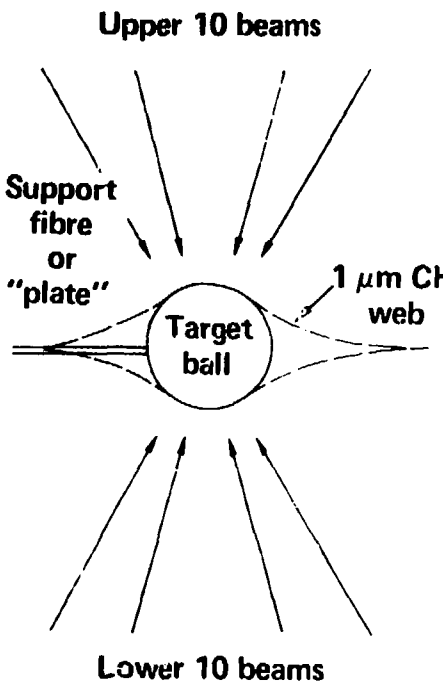

ρ(g/cm^3)	Mat'l	R(μm)
1.8	$CF_{1.4}$	90
2.2	Glass	75
0.01	DT + Ar (seed)	70

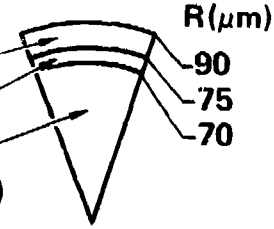

Performance parameters

τ_l = 200 ps (Gaussian, FWHM)

E_{inc} = 4 kj

$I_{inc} = 1 - 3 \times 10^{16}$ W/cm^2

F_{abs} = 20%

F_{hot} = 90%, T_{hot} = 35 - 60 keV

$Y = 6 \times 10^8$

ρ_{dt} = 15 × l.d.

02-30-1079-4336

HIGH ENERGY X-RAY EMISSION SUGGEST $T_{hot} \sim 30$ keV, $f_{hot} \sim 0.5$

- **Significant uncertainty: angular emission modulation**

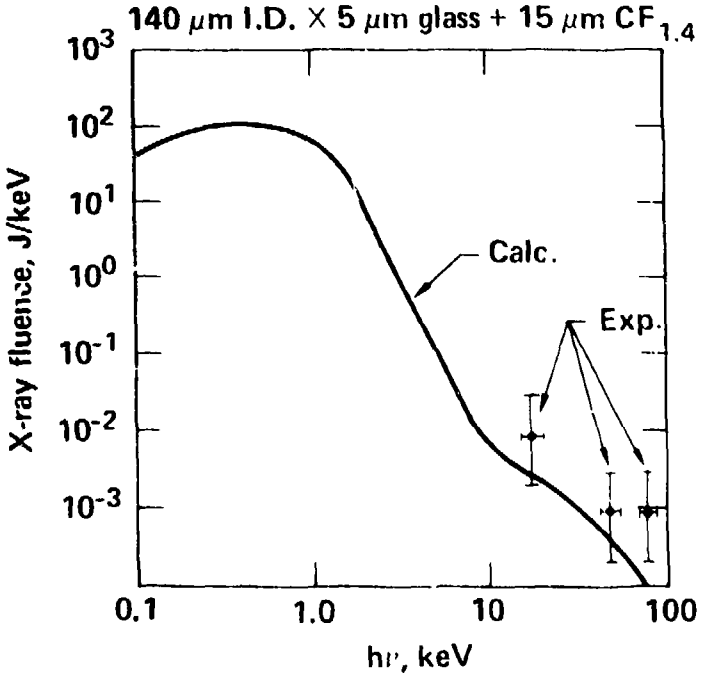

τ_l = 200 ps
E_{inc} = 4 kj
E_{abs} = 700 j

Calc.

T_{hot}:
Source = 35 keV
X-rays = 21 keV
f_{hot} = 0.90

Exp.

$T^{x}_{hot} = 24 \pm 5$ keV
$f_{hot} \sim 0.5$

50-60-1079-4351

SHIVA "10×" DESIGN SHOWS MODERATE BRILLOUIN SCATTERING

- Small sphere
- High intensity

$$I \sim 10^{16}\ W/cm^2$$

$$\frac{\nu_o}{\nu_e} \sim 1 - 2,\ \frac{T_e}{ZT_i} \lesssim 1$$

$\Longrightarrow$ Significant density step at critical

$$Q_{ss} \simeq \left(\frac{n_p}{n_c}\right)\left(\frac{\nu_o}{\nu_e}\right)^2\left(\frac{L}{\lambda_o}\right) \simeq \left(\frac{1}{3}\right)(1)^2(20) \simeq 6$$

- Expect ~50% scatter
- Experiment shows 20% absorption, nominal considering incidence angle and polarization

RADIUS VS TIME FOR "10 · " BALL TARGET SHOWS EARLY ABLATION FOLLOWED BY PUSHER DECOMPRESSION

- **A "swelling pusher" implosion**

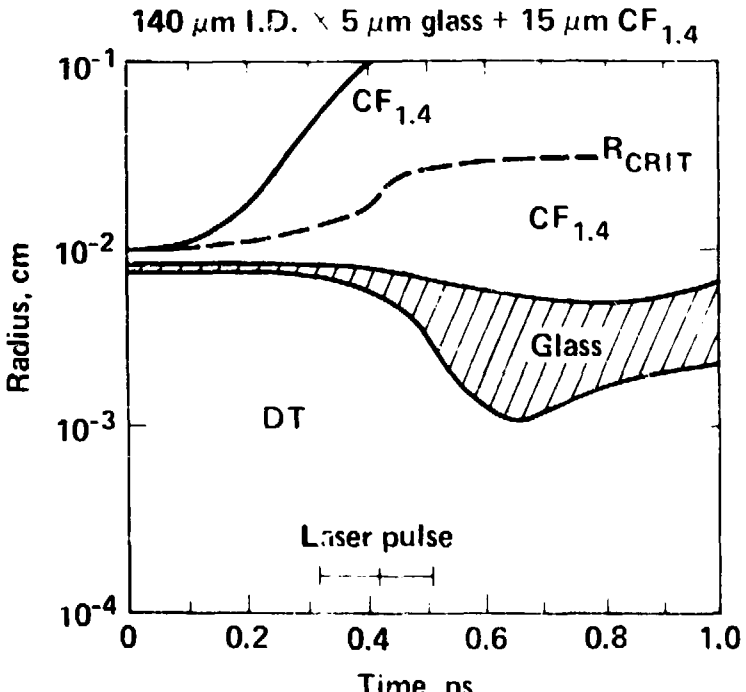

τ_l = 200 ps
E_{inc} = 4 kj
E_{abs} = 700 j

50-60-1079-4350

PROFILES AT PEAK OF LASER PULSE SHOW "10×" DESIGN EXHIBITS SIGNIFICANT PUSHER BURN-THROUGH

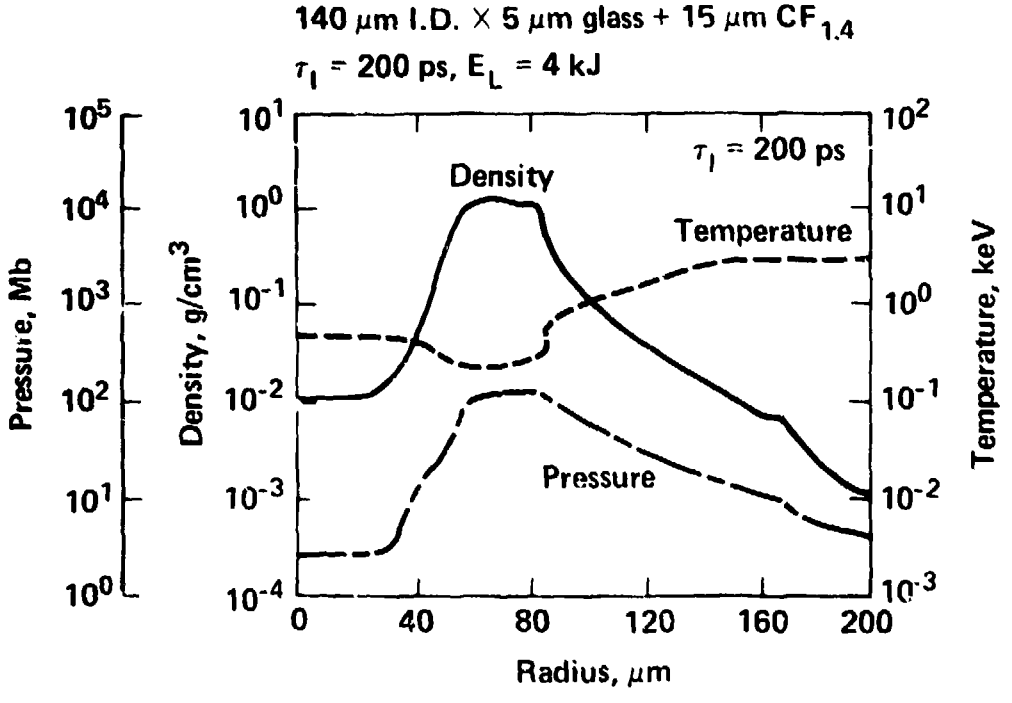

50-60-1079-4349

STAGNATION HISTORY SHOWS SEQUENCE OF TIMES FOR BURN, MIX AND PEAK ρ AND ρr FOR "10 ×" DESIGN

- Implosion timing depends upon capsule, drive, preheat

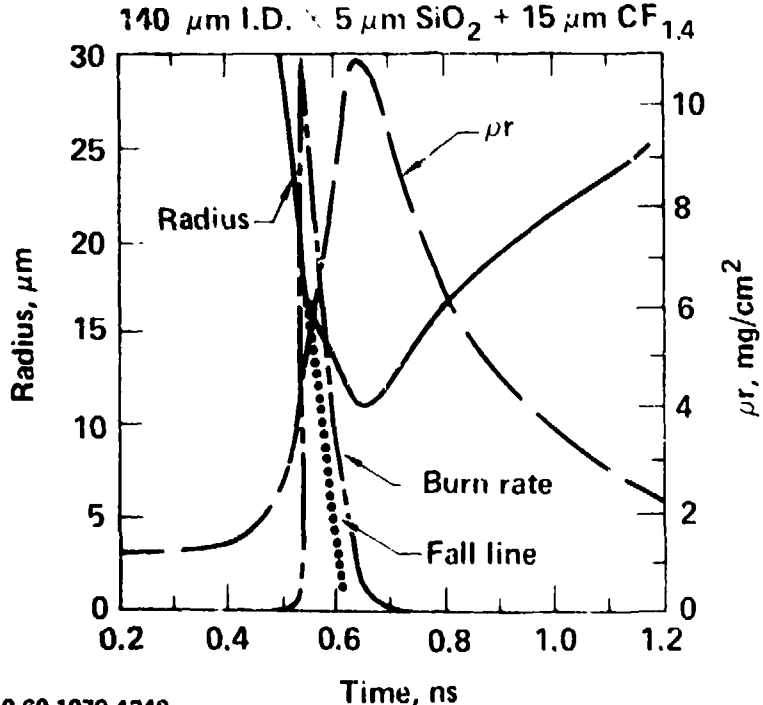

τ_i = 200 ps

E_{inc} = 4 kj

E_{ABS} = 700 j

$$Y_{mix} \simeq \frac{1}{2} Y_{no\text{-}mix}$$

50-60-1079-4348

CALCULATED PROFILES SHOW INCOMPLETE PUSHER ASSEMBLY AT PEAK COMPRESSION

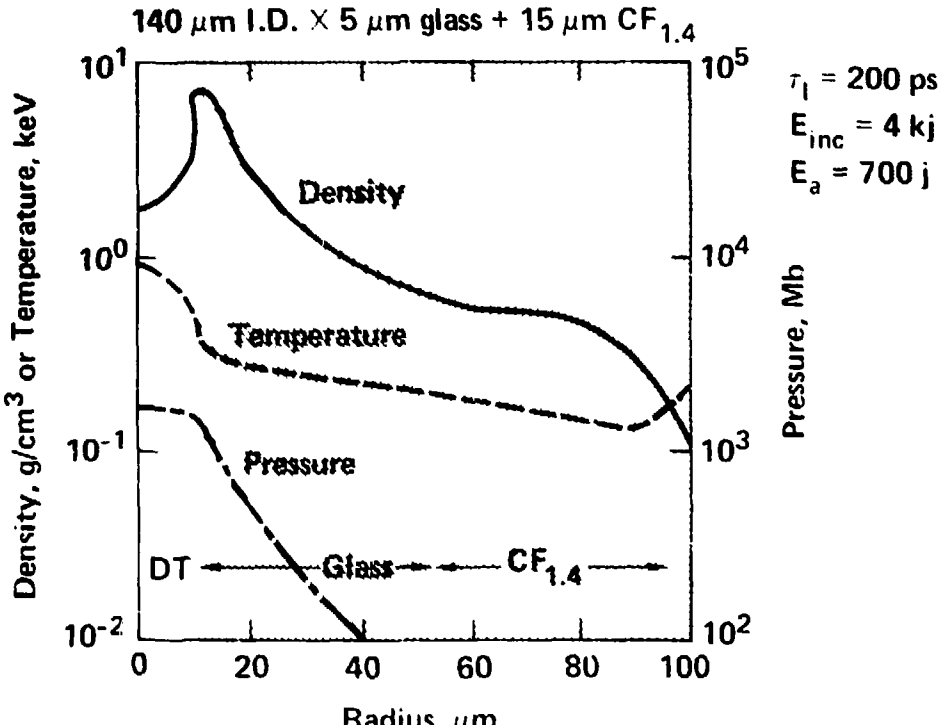

50-60-1079-4347

DT ADIABATS FOR 10 - 100 · TARGET DESIGNS

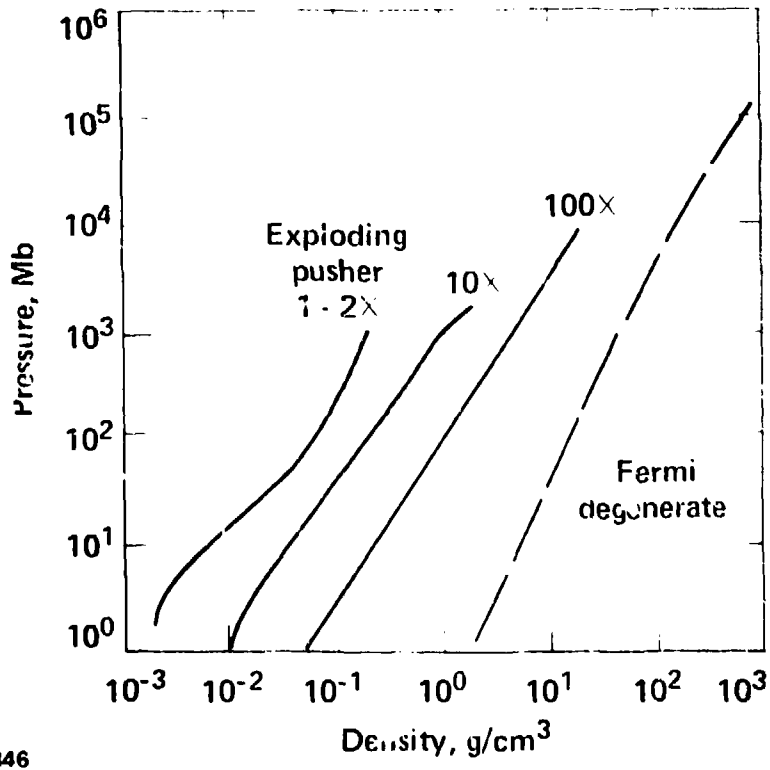

50-60-1079-4346

COMPARISON OF CALCULATED AND MEASURED NEUTRON YIELDS

140 μm I.D. X 5 μm glass + 15 μm $CF_{1.4}$, 0.01 g/cm^3 DT fill
τ_L = 200 ps

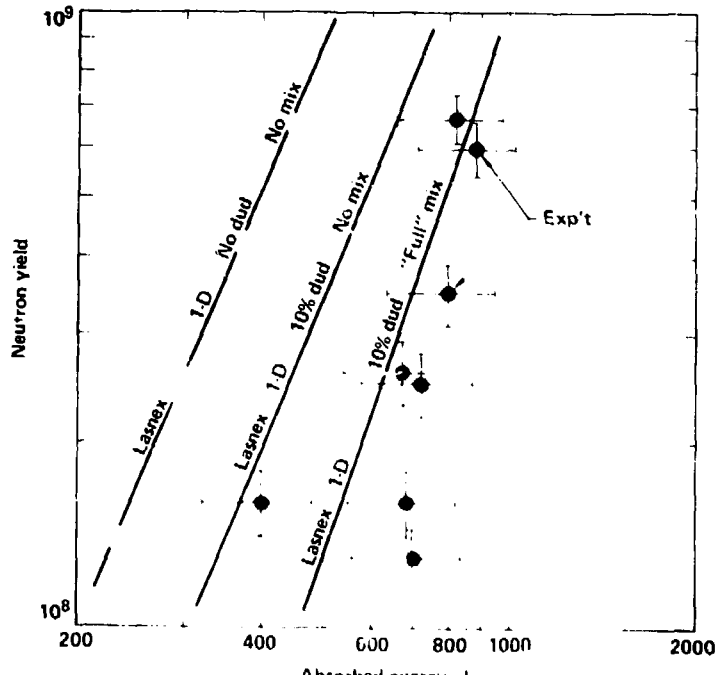

50-60-1079-4558

2-D CALCULATION WITH INHIBITED TRANSPORT SHOWS MODERATELY AS\ MMETRIC IMPLOSION

140 μm I.D. X 5 μm glass + 15 μm $CF_{1.4}$, 0.01 g/cm^3 DT fill

τ_L = 200 ps, E_L = 4.0 kJ

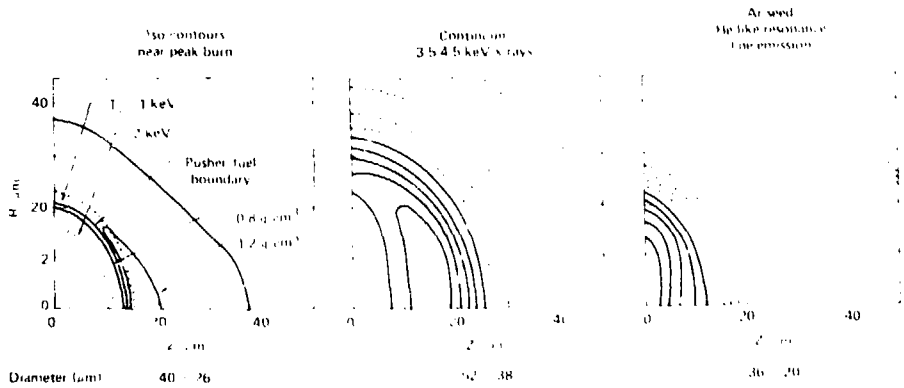

3 METHODS USED TO DIAGNOSE "IOX" IMPLOSIONS

- X-ray imaging
- Imaging of Ar seed line emission
- Radiochemical pusher activation

EVEN FOR "IOX" TARGET, DETAILS OF X-RAY IMAGE DEPEND STRONGLY ON DETAILED IMPLOSION CHARACTERISTICS

Strong competition between fuel and pusher emission controlled by:

- Photon frequency imaged
- Pusher optical depth: $\kappa\rho\Delta x \sim 1$
- High-Z seeded and/or mixed into fuel
- Space/time dependence of $\bar{Z}$, T_e, n_e
- Implosion asymmetry

50-60-1079-4344

"10X" CALCULATIONS SHOW X-RAY IMAGE FWHM COMPARABLE WITH EXPERIMENTAL IMAGES

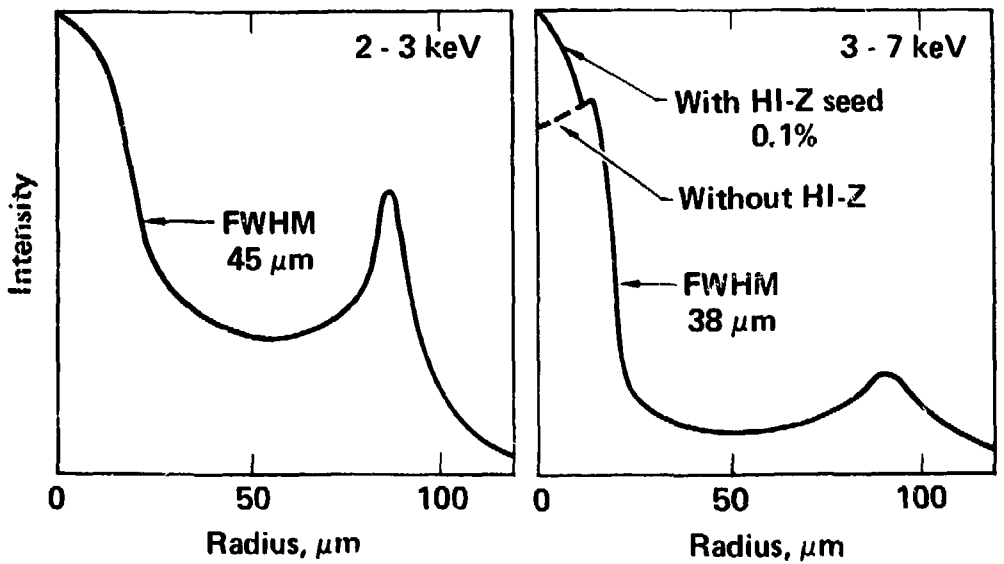

- Details are very model dependent

50-60-1079-4343

1.5-2.5 keV X-RAY MICROSCOPE IMAGES

Heating symmetry is significantly improved by focusing energy on thin plate

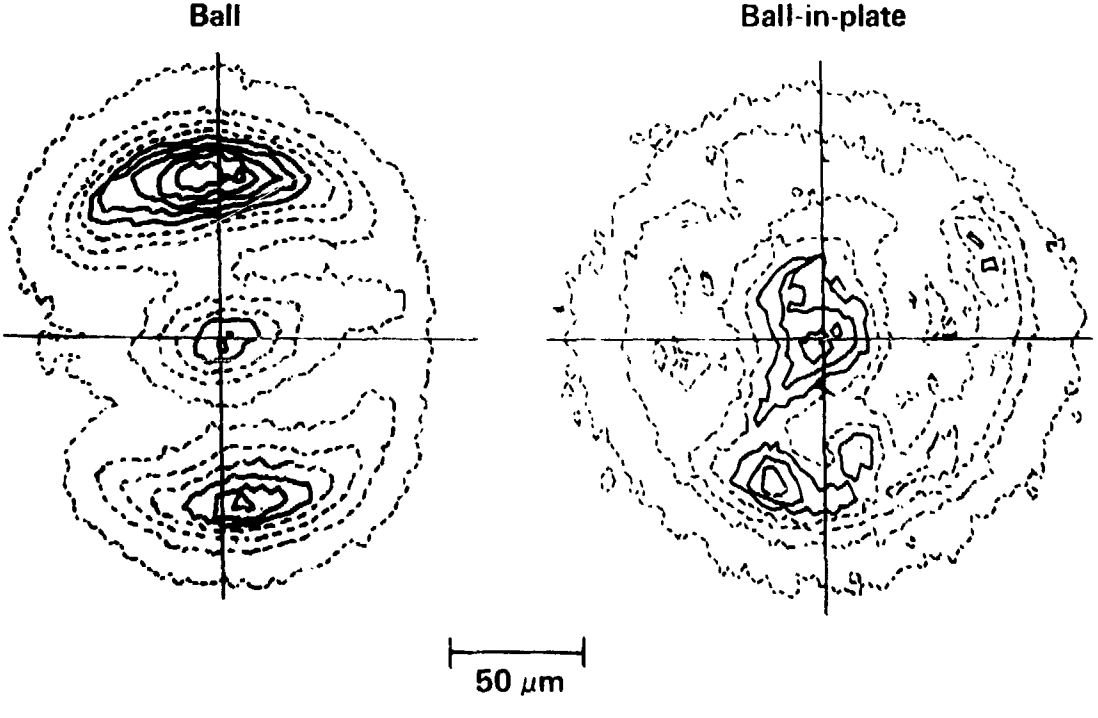

50-60-1079-4353

3.5 - 4.5 keV X-RAY MICROSCOPE IMAGES

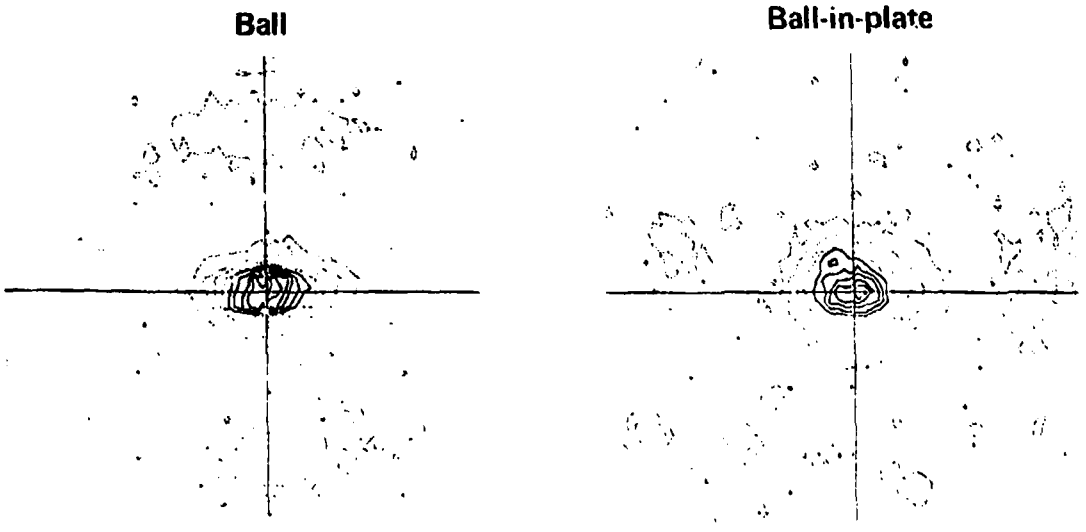

Symmetry of stagnated core is improved using ball-in-plate configuration

50-60-1079-4352

IMAGE OF Ar LINE EMISSION FROM COMPRESSED CORE INDICATES FUEL DIMENSION

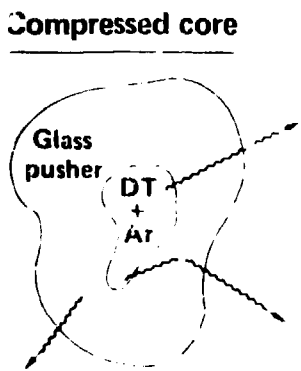

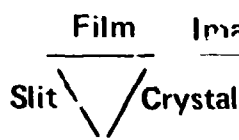

- He-like Ar excited at stagnation
  $T_E \sim 0.6 - 1.0$ keV
  $N_E \sim 10^{23} - 10^{24}$ cm^{-3}
  $I_O \sim 10^{16} - 10^{17}$ keV/keV

- Background
  Si free-bound
  Corona emission
  $I_B \sim 3 \times 10^{15}$ keV/keV

- Transport through pusher
  Si K-shell bound-free
  $\rho R)_{SiO_2} \sim 0.005$ g/cm^2
  Attenuation 5 - 15 x
  $I_S \sim 10^{15} - 10^{16}$ keV/keV

CORRECTIONS TO SIZE OF Ar LINE IMAGE ARE MODERATE FOR SHIVA "10X" IMPLOSIONS

Emission peaks before maximum compression

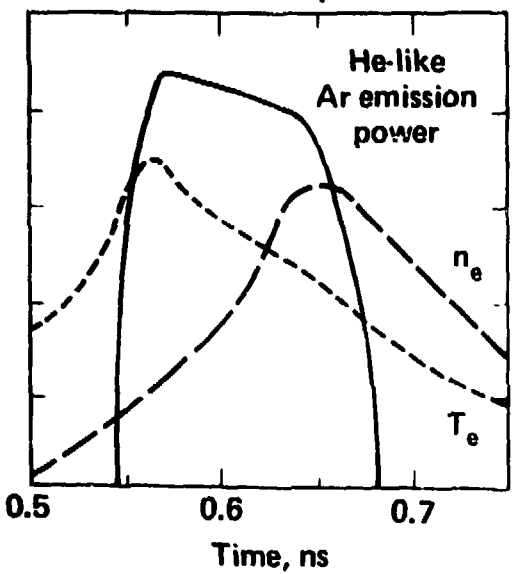

Optical depth variation has small effect on image size

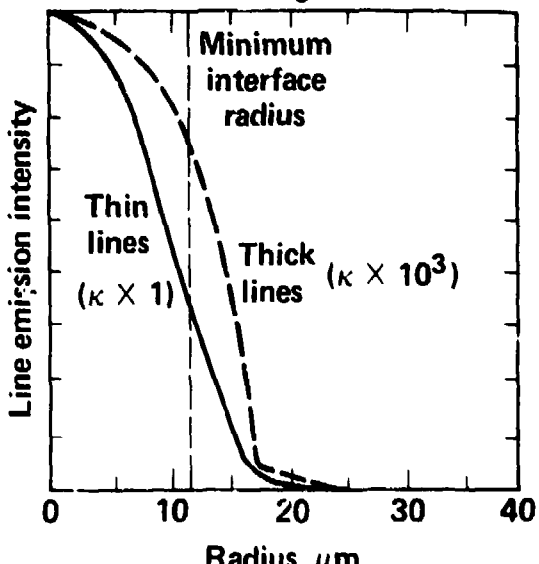

- $n_{e\text{-peak}} \simeq 1{\cdot}2 \cdot n_{e\text{-Ar}}$
- Implosion sphericity must be determined

50-60 1079-4341

1-D IMAGE OF He-LIKE Ar RESONANCE LINE FROM EXPERIMENT IS CONSISTENT WITH 2-D CALCULATION

140 μm I.D. X 5 μm glass + 15 μm $CF_{1.4}$, 0.01 g/cm^3 DT

$\tau_{l.}$ = 200 ps, E_L = 4.0 kJ

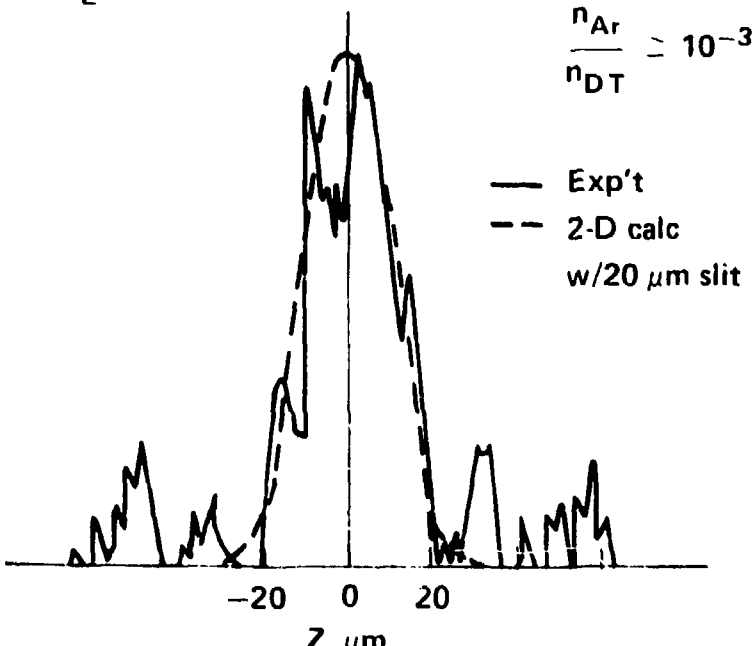

50-60-1079-4559

RADIOCHEMICAL ACTIVATION OF PUSHER OR SEED MATERIAL DETERMINES ρR AT "BURN" TIME

Compressed core

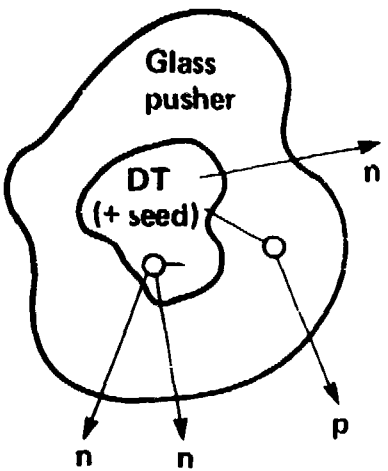

Reactions

- **Pusher**

  $^{28}Si + n \quad ^{28}Al + p$

  $^{28}Al \rightarrow {}^{28}Si, \beta, \gamma$

  Diagnostic threshold: $N(\rho R)_p \sim 10^5$

- **Fuel seed**

  $^{79}Br + n \quad ^{78}Br + 2n$

  $^{78}Br \rightarrow {}^{78}Se, \beta^+$

  Diagnostic threshold: $N(\rho R)_f \sim 3 \times 10^5$

$$\frac{\text{Activation yield}}{\text{Neutron yield}} \sim \rho R)_{\text{eff}}, \sim n\tau$$

50-60-1079-4340

SIMPLE MODEL ILLUSTRATES BASIC RELATIONSHIP BETWEEN PUSHER ρR AND FUEL DENSITY

- Initial conditions

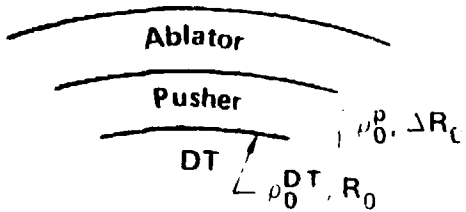

- Configuration at burn

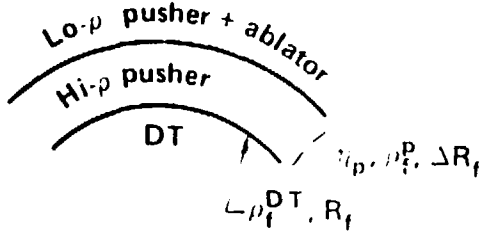

η_p = pusher mass fraction compressed

- Assume 1-D spherical geometry
- Thin shell pusher
- Final mass = η_p · initial mass

$$4\pi R_f^2 \rho_f^p \Delta R_f = \eta_p 4\pi R_0^2 \rho_0^p \Delta R_0$$

determines R_0/R_f

$$\rho_f^{DT} = \left(\frac{R_0}{R_f}\right)^3 \rho_0^{DT}$$

$$\rho_f^{DT} = \left[\frac{(\rho\Delta R)_f^p}{\eta_p (\rho\Delta R)_0^p}\right]^{3/2} \rho_0^{DT}$$

- Cleanest result if $\eta_p = 1$

1-D MODEL DEPENDENCE ARISES THROUGH VARIATIONS IN IMPLOSION/STAGNATION DYNAMICS

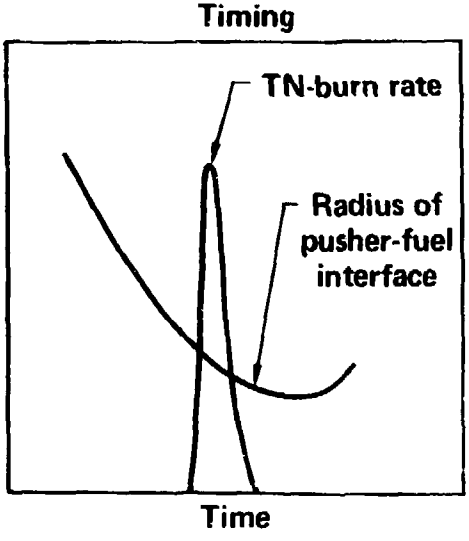

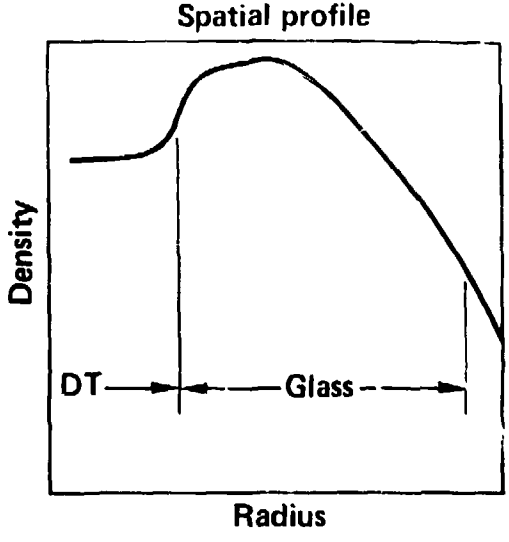

$$\text{Heating rate} \propto P\frac{dV}{dt}$$

$$\text{Cooling rate} \propto \kappa \nabla T_e$$

Detailed features of preheat/ablation/convergence

2-D EFFECTS ARISE THROUGH IMPLOSION ASYMMETRY AND FLUID INSTABILITY/MIXING OF PUSHER AND FUEL

Asymmetry

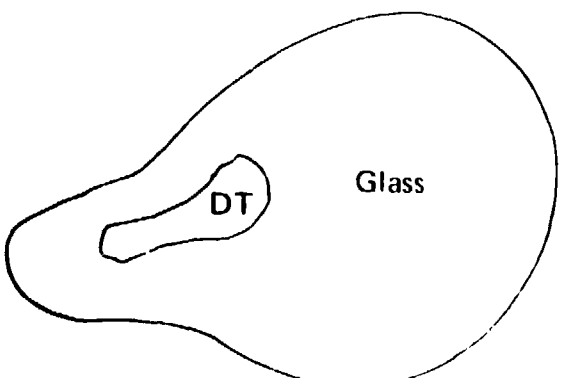

Instability/turbulent mix

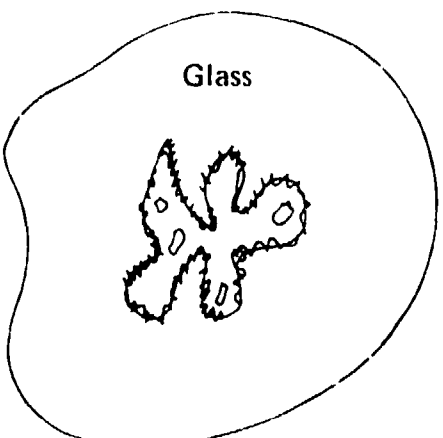

Distortions need to be quite large to significantly affect $\rho)_F$ vs $\rho\Delta R)_P$

50-60-1079-4338

CALCULATIONAL SENSITIVITY TESTS SHOW DEPENDENCE OF YIELD, ρR ON PHYSICS MODEL

τ_L = 200 ps, 140 μm I.D. × 5 μm glass + 15 μm $CF_{1.4}$, 0.01 g/cm^3 DT fill

Model variations: E_A, T_{hot}, f_e, r_e τ_{ei}, glass EOS

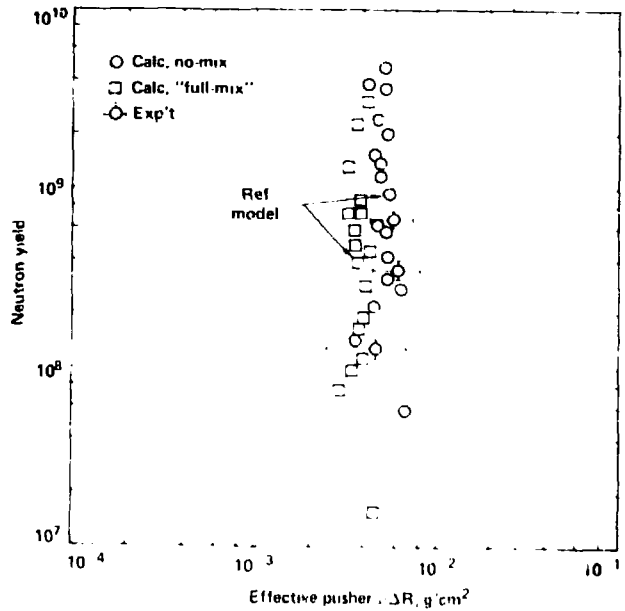

50-60-1079-4561

RESULTS OF SENSITIVITY STUDY SHOW α_F CAN BE INFERRED FROM $(\rho\cdot\Delta R)_p$ WITH ~ 2× UNCERTAINTY

140 μm I.D. × 5 μm glass + 15 μm $CF_{1.4}$, 0.01 g/cm³ DT fill

τ_L = 200 ps

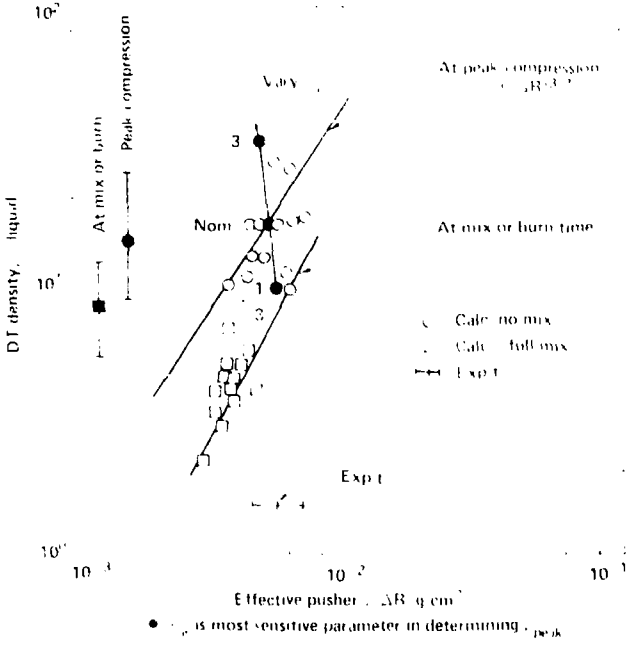

50-60-1079-4562

LONGER PULSES AND THICKER ABLATORS LEAD TO HIGHER DENSITY

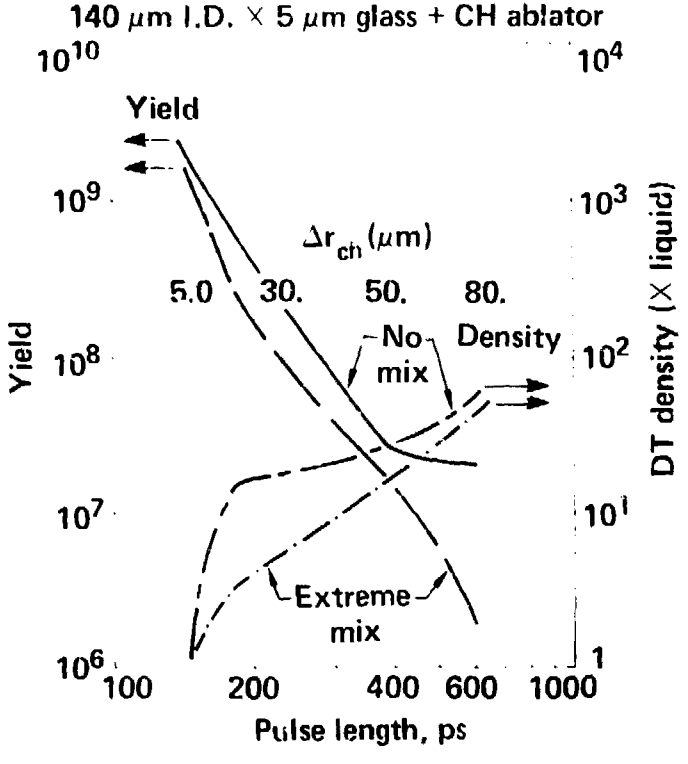

But sensitivity to preheat, symmetry, and mix increases

50-60-1079-4037